Spectroscopic properties and intense red-light emission of (Ca, Eu, M)WO$_4$ (M = Mg, Zn, Li)

Shikao Shi [a,*], Xingren Liu [b], Jing Gao [a], Ji Zhou [c]

[a] *College of Chemistry and Materials Science, Hebei Normal University, Shijiazhuang 050016, PR China*
[b] *Changchun Institute of Optics, Fine Mechanics and Physics, Chinese Academy of Sciences, Changchun 130021, PR China*
[c] *Department of Materials Science & Engineering, Tsinghua University, Beijing 100084, PR China*

Abstract

The red-emitting phosphors of (Ca, Eu, M)WO$_4$ (M = Mg, Zn, Li) were prepared through solid-state reactions, and their spectroscopic properties were studied. After the addition of a small amount of Mg^{2+}, Zn^{2+} or Li$^+$ in (Ca, Eu)WO$_4$, the red-light emission intensity of Eu^{3+} increases obviously. In the luminescence spectra of the phosphors, the predominant transition emission is $^5D_0 \rightarrow {}^7F_2$ (616 nm), whereas the other emissions are very weak. The excitation spectra are composed of interweaved ligand-to-metal charge-transfer bands (CTB) of W^{6+}–O^{2-} and Eu^{3+}–O^{2-}, and a few 4f excitation transitions of Eu^{3+}. Among the 4f excitation transitions of Eu^{3+}, there are three strong excitation lines corresponding to $^7F_0 \rightarrow {}^5L_6$, $^7F_0 \rightarrow {}^5D_2$ and $^7F_0 \rightarrow {}^5D_1$ transitions, whose relative excitation intensity ratio is seriously affected when Li$^+$ doped in the host. The new phosphors may be applied as red-emitting phosphors for white light emitting diodes.
© 2007 Elsevier B.V. All rights reserved.

Keywords: Spectroscopic properties; Eu^{3+} ion; CaWO$_4$; f–f transitions

1. Introduction

Due to the rapid rises of new semiconductor solid-state lighting devices—white light emitting diodes (LEDs) since the end of the last century, tremendous achievements have been made in the development of key materials and technology including semiconductor photoelectron, lighting project and new luminescent materials. White LED is a remarkable resource because it is environment-friendly and energy-saving in the 21st century. Therefore, it is promising for the market applications [1]. One of the most common methods to assemble white LED is to combine an InGaN blue LED chip with a yellow-emitting phosphor YAG:Ce^{3+}, which has been commercialized [2,3]. However, there exist at least two drawbacks in this combination. Firstly, the overall efficiency is decreased rapidly when the correlated color temperature of the device is low. Secondly, the output light is deficient in the red region of the visible light spectrum. The other promising white LED is to use red, green and blue light-emitting phosphors coated on the near-UV LED chip, which is a focus in material and luminescence research nowadays. The commercialized products on LED with near-UV (390–410 nm) excitation are available. Nevertheless, the red-emitting phosphor that can be effectively excited with the near-UV light is still lacking. The luminescent efficiency of Y$_2$O$_2$S:Eu^{3+} phosphor used in color television is very low under near-UV irradiation. In consequence, much attention has been paid to make superior red phosphor for white LED.

Recently, the trivalent europium ions activated tungstates and molybdates are shown to have efficient red-light emission in the near-UV irradiation. Neeraj et al. [4] reported the emission intensity of the phosphor NaY$_{0.95}$Eu$_{0.05}$(WO$_4$)$_{2-x}$(MoO$_4$)$_x$ with scheelite structure is 7.28 times of Y$_2$O$_2$S:Eu, Sm excited at 395 nm, while the emission intensity of NaY$_{0.95}$Eu$_{0.05}$(WO$_4$)$_2$ is just 3.25 times of Y$_2$O$_2$S:Eu, Sm excited at 395 nm. Similar red phosphor AgLa$_{0.95}$Eu$_{0.05}$(WO$_4$)$_{2-x}$(MoO$_4$)$_x$ was reported by Sivakumar and Varadaraju [5], and NaLa$_{1-x}$R$_x$(MoO$_4$)$_2$ (R = Eu, Sm) was also prepared by Wang et al. [6]. In addition, the phosphor Ca$_{1-2x}$Eu$_x$Li$_x$MoO$_4$ prepared by Jing and co-workers [7] has shown superior luminescence efficiency compared with that of (Ca, Eu)MoO$_4$ reported in the earlier paper [8].

Table 1
Composition and relative intensities of (Ca, Eu, M)WO$_4$ (M = Li, Mg, Zn)

Sample no.	Composition	I_{616}	I_{616}/I_{592}
01	CaWO$_4$	–	–
02	Ca$_{0.76}$Eu$_{0.24}$WO$_4$	100	1:0.138
03	Ca$_{0.70}$Eu$_{0.24}$Mg$_{0.06}$WO$_4$	145	1:0.116
04	Ca$_{0.70}$Eu$_{0.24}$Zn$_{0.06}$WO$_4$	151	1:0.105
05	Ca$_{0.52}$Eu$_{0.24}$Li$_{0.24}$WO$_4$	147	1:0.117

CaWO$_4$ with the scheelite structure was first used as X-ray luminescent materials as soon as it was found in 1896 [9], which has been used all the same in the following whole century. Typical self-activated CaWO$_4$ is a high-efficiency material emitting blue light under X-ray, electron beam and UV irradiation [10,11]. Between the 1970s and 1980s, Powell and co-workers [11,12] had studied the luminescent properties and energy transfer of CaWO$_4$ and CaWO$_4$:Eu^{3+} systems. Nevertheless, the change of Eu^{3+} 4f energy transition excitation spectra has been neglected for a long time. To date, it is still necessary to make a further cognition about the excitation spectra of Eu^{3+} in tungstates and molybdates. In this paper, the spectroscopic properties of Eu^{3+} were studied in CaWO$_4$ doped with Li$^+$, Mg^{2+} or Zn^{2+} under UV–visible light irradiation, especially the influence of the Eu^{3+} 4f excitation spectra (monitored at 616 nm) at 290–550 nm on the luminescence intensity of Eu^{3+}.

2. Experiments

Undoped and doped CaWO$_4$ samples were prepared by the solid-state reaction. The starting materials WO$_3$ (99.9%), CaCO$_3$ (G.R.), Eu$_2$O$_3$ (99.99%), Li$_2$CO$_3$ (A.R.), MgO (A.R.) and ZnO (A.R.) were blended in appropriate stoichiometric ratio (Table 1). These powders were ground thoroughly in an agate mortar, and then the heterogeneous mixture was put into an alumina crucible and calcined in a muffle furnace at 1070–1100 °C for 3 h in air. When more Li$_2$CO$_3$ was added, the calcination temperature should be decreased properly. The final samples are white powders.

The crystal structure of the sample was identified by X-ray diffraction (XRD), which was recorded on a Rigaku D/max-rb X-ray diffraction running Cu Kα radiation at 40 kV and 250 mA. A VARIAN Cary-Eclipse fluorescence spectrometer was used to detect the excitation and emission spectra of the samples at ambient temperature.

3. Results and discussion

3.1. Structure of the phosphors

Fig. 1 gives the XRD patterns of CaWO$_4$ (01), (Ca, Eu)WO$_4$ (02) and (Ca, Eu, Zn)WO$_4$ (04). The XRD patterns of (Ca, Eu, Mg)WO$_4$ (03) and (Ca, Eu, Li)WO$_4$ (05) are not shown, due to their similarity with (Ca, Eu, Zn)WO$_4$ (04). All the five compounds are isostructural and belong to the tetragonal system of Scheelite type. In this structure, W^{6+} occupies the tetrahedral sites constructed with O^{2-}, composing WO$_4{}^{2-}$ anion complex.
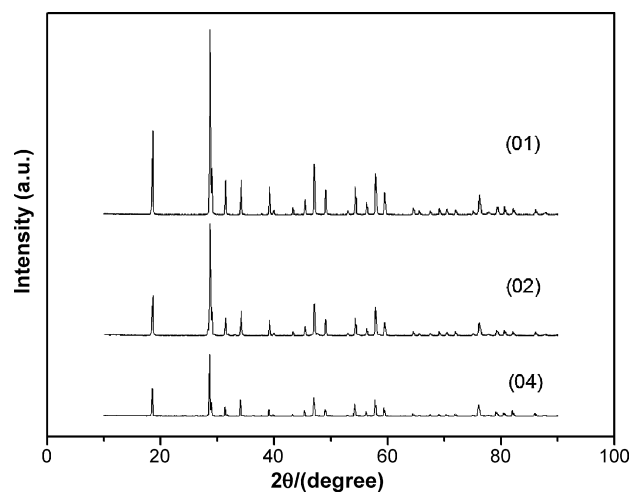

Fig. 1. XRD patterns of CaWO$_4$ (01), (Ca,Eu)WO$_4$ (02) and (Ca,Eu,Zn)WO$_4$ (04).

Ca^{2+} is eight-coordinated with O^{2-}, forming a distorted cube. The dopant Eu^{3+} or other metal ions occupy the Ca^{2+} site. With the increase of the dopant concentration, the characteristic diffraction intensity decreases obviously, but there is no shift in the peak location, indicating that the doped Eu^{3+} or other metal ions have little influence on the host structure.

3.2. Emission spectra of Eu^{3+}

Fig. 2 shows the emission spectra of four samples (No. 02, 03, 04 and 05) excited by near-UV (395 nm) at ambient temperature. Their emission spectra are similar, corresponding to typical 4f levels specific transitions of Eu^{3+}. The characteristic emission of WO$_4{}^{2-}$ in CaWO$_4$:Eu^{3+} is quenched absolutely and only red-light emission of Eu^{3+} appears. The strong emission peak around 616 nm is due to the electric dipole energy transition of $^5D_0 \rightarrow {}^7F_2$. The weak emission in the vicinity of 592 nm is ascribed to the magnetic dipole transition of $^5D_0 \rightarrow {}^7F_1$. The ratio of the two emission intensities (I_{616}/I_{592}) and the relative
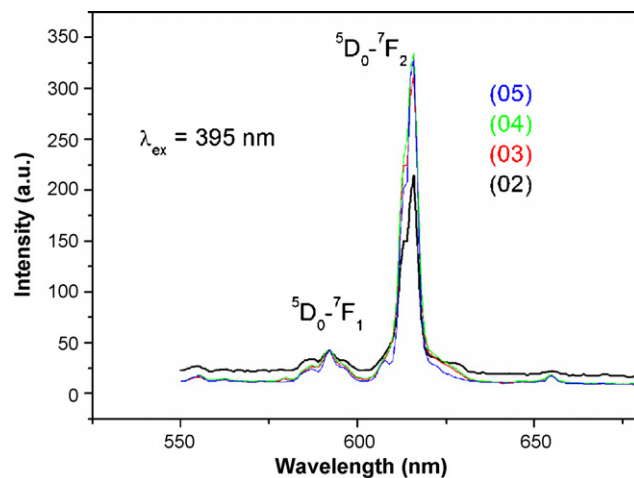

Fig. 2. Emission spectra of (Ca, Eu)WO$_4$ (02), (Ca, Eu, Mg)WO$_4$ (03), (Ca Eu, Zn) WO$_4$ (04) and (Ca Eu, Li)WO$_4$ (05) excited at 395 nm.
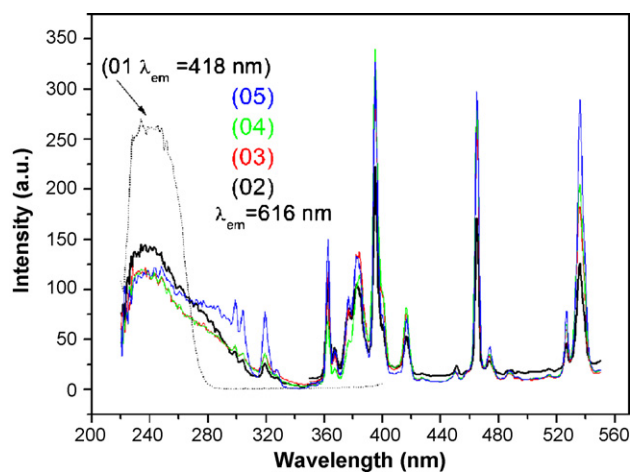
Fig. 3. Excitation spectra of $CaWO_4$ (01), (Ca, Eu)WO_4 (02), (Ca, Eu, Mg)WO_4 (03), (Ca Eu, Zn) WO_4 (04) and (Ca Eu, Li)WO_4 (05).

Table 2
Transition energies of Eu^{3+} in the excitation spectra of (Ca, Eu, M)WO_4 (M = Mg, Zn, Li) at ambient temperature

Transitions	Excitation maximum (nm)
$^7F_0 \to {}^5F_4$	298
$^7F_0 \to {}^5F_2$	304
$^7F_0 \to {}^5H_3$	319
$^7F_2 \to {}^5H_4$	327
$^7F_0 \to {}^5D_4$	363[a], 367
$^7F_0 \to {}^5L_7$	377, 382[a], 385
$^7F_0 \to {}^5L_6$	395[a], 400
$^7F_0 \to {}^5D_3$	416
$^7F_0 \to {}^5D_2$	465
$^7F_1 \to {}^5D_2$	474
$^7F_2 \to {}^5D_2$	486
$^7F_0 \to {}^5D_1$	527, 536[a]

[a] Represents the predominant line in the group.

emission intensities of the four samples at 616 nm (I_{616}) are presented in Table 1, respectively. It is evidently that the $^5D_0 \to {}^7F_2$ transition emission intensity of Eu^{3+} increases significantly with incorporation of Mg^{2+}(03), Zn^{2+}(04), Li^+(05) ions into $CaWO_4$. The $^5D_0 \to {}^7F_2$ transition is hypersensitive to the local environment of the Eu^{3+}. It is generally a forced electric dipole transition whose intensity depends on coupling with either odd terms in the crystal field or odd parity lattice vibration modes. In the tetragonal system $CaWO_4$, Eu^{3+} ions substitute partially for Ca^{2+} ions and have S_4 site symmetry. Nevertheless, the emission spectra are dominated by the electric dipole transition $^5D_0 \to {}^7F_2$ of Eu^{3+}, which manifests that Eu^{3+} ions occupy the asymmetry center site [11]. The doping with Mg^{2+}, Zn^{2+} or Li^+ into $CaWO_4$ results in the enhancement of I_{616}/I_{592} (see Table 1). This implies that the crystal field environment of Eu^{3+} is modified and more Eu^{3+} ions occupy the asymmetry center sites. As a result, the $^5D_0 \to {}^7F_2$ transition emission intensity increases dramatically and the color purity of the red light is improved. In addition, other radiation transition emissions of Eu^{3+} 4f high energy (such as $^5D_{1,2}$) are very weak.

3.3. Charge-transfer bands (CTB)

Fig. 3 shows the excitation spectra of the samples at ambient temperature. The excitation spectrum (monitored at 418 nm) of pure $CaWO_4$ (01) shows a strong broadband at short-wavelength UV region. The excitation curve has peaks at about 240 nm, which is ascribed to a charge-transfer band of W^{6+}–O^{2-} within the WO_4^{2-} group (abbreviated as CTB(W^{6+})).

The Eu^{3+} excitation spectra (monitored at 616 nm) of the samples (02, 03, 04 and 05) are quite similar, consisting of two interweaved broad excitation bands in the vicinity of 200–340 nm and sharp 4f transition excitation lines of Eu^{3+}, which cover the ranges from long-wavelength UV to visible green-light region (300–550 nm). The excitation band ($\lambda_{max} = 235$–240 nm) at short-wavelength UV region (200–280 nm) overlaps with another excitation band ($\lambda_{max} \sim 285$ nm) at middle-wavelength UV region (250–340 nm). The profile and peaks of this excitation spectra

under short-wavelength UV match well with that of CTB(W^{6+}). With the introduction of Mg^{2+} and Zn^{2+} into $CaWO_4$, the excitation peaks ($\lambda_{max} \sim 235$ nm) of CTB(W^{6+}) shift to the short-wavelength side in a small amount. However, the same result is not observed in the (Ca, Eu, Li)WO_4 (05). In the excitation spectra of (Ca, Eu)WO_4 and (Ca, Eu, M)WO_4 (M = Mg, Zn, Li), the relative intensities of CTB(W^{6+}) are much weaker than that of pure $CaWO_4$. The relative weak excitation bands at the UV region ($\sim$285 nm) correspond to the CTB(Eu^{3+}) of Eu^{3+}–O^{2-}. This phenomenon is similar to CTB (260 nm) of W^{6+}–O^{2-} and CTB (310 nm) of Eu^{3+}–O^{2-} in $Eu_2(WO_4)_3$ [13].

In luminescent materials, there exist two kinds of couplings between luminescent center and crystal lattice. One is the strong coupling (such as WO_4^{2-} and MoO_4^{2-} groups) with high Huang-Rhys factor. The other belongs to the weak coupling (such as Eu^{3+} and Tb^{3+} ions) with relatively low Huang-Rhys factor [14,15]. In $CaWO_4$:Eu^{3+}, the strong coupling of CTB(W^{6+}) is predominant, whereas the weak coupling of CTB(Eu^{3+}) is subordinate. When CTB(W^{6+}) is excited, the energy absorbed from charge-transfer state is efficiently transferred to Eu^{3+} ion by a non-radiative mechanism, and generate red-light emission of the $^5D_0 \to {}^7F_J$ transition of Eu^{3+}. Simultaneously, the blue-light emission of the self-activated $CaWO_4$ is quenched.

3.4. The 4f excitation transitions of Eu^{3+}

Chronically, the main study on the excitation spectra of Eu^{3+} is the charge-transfer band of Eu^{3+}–O^{2-}, while the excitation spectra variation of Eu^{3+} 4f energy transition (290–550 nm) is neglected. Here, we try to make a brief analysis on this aspect.

There are groups of sharp excitation lines of Eu^{3+} 4f levels in the wide range of excitation spectra from 290 nm to 550 nm, which are listed in Table 2. Among these excitation transitions, $^7F_0 \to {}^5L_6$ (395 nm), $^7F_0 \to {}^5D_2$ (465 nm) and $^7F_0 \to {}^5D_1$ (536 nm) lines are the most intense ones.

The excitation peaks of these samples (02, 03, 04 and 05) are practically identical, coinciding with other tungstates [13], because the f–f transitions are in little measure affected in

the crystal field environment. However, the intensity differences of the excitation spectra can be clearly observed from Fig. 3. The relative excitation intensities of Eu^{3+} monitored at 616 nm ($^5D_0 \rightarrow {}^7F_2$) vary with different excitation wavelength. Especially, the intensities of $^7F_0 \rightarrow {}^5D_2$ (465 nm) and $^7F_0 \rightarrow {}^5D_1$ (536 nm) compared with $^7F_0 \rightarrow {}^5L_6$ (395 nm) are enhanced in the sequence of 02 < 03(Mg) < 04(Zn) < 05(Li). For example, in $Ca_{0.76}Eu_{0.24}WO_4$ (02), the ratios of relative excitation intensities (I_{395}:I_{465}:I_{536}) of Eu^{3+} ($\lambda_{em} = 616$ nm) are 1:0.76:0.55. Whereas, the ratios of relative excitation intensities in $Ca_{0.70}Eu_{0.24}Mg_{0.06}WO_4$ are changed to 1:0.87:0.59. When Li^+ doped in the host, the ratios of relative excitation intensities are 1:0.93:0.91, which means that the excitation transition of the blue (465 nm) and green (536 nm) lines are greatly enhanced. Another noticeable feature is that, in (Ca, Eu, M)WO_4 (M = Mg, Zn, Li) systems, the relative intensities of Eu^{3+} 4f excitation lines ($^7F_0 \rightarrow {}^5L_6$, $^7F_0 \rightarrow {}^5D_2$ and $^7F_0 \rightarrow {}^5D_1$) transcend the charge-transfer bands of W^{6+}–O^{2-} and Eu^{3+}–O^{2-}. In addition, the 4f energy levels excitation transition lines $^7F_0 \rightarrow {}^5F_4$ (298 nm), $^7F_0 \rightarrow {}^5F_2$ (304 nm) and $^7F_0 \rightarrow {}^5H_3$ (319 nm) of (Ca, Eu, Li)WO_4 (05) can be evidently observed at ambient temperature.

4. Conclusions

The incorporation of Mg^{2+}, Zn^{2+} or Li^+ ions into the $CaWO_4$ crystalline lattice makes the red-light emission intensity of Eu^{3+} increases obviously. In the emission spectra, the strongest emission is the electric dipole transition red emission $^5D_0 \rightarrow {}^7F_2$ (616 nm), while the magnetic dipole transition orange emission $^5D_0 \rightarrow {}^7F_1$ (592 nm) is subordinate. The wide excitation bands of (Ca, Eu, M)WO_4 in the short-wavelength UV region are composed of interweaved ligand-to-metal charge-transfer bands (CTB) of W^{6+}–O^{2-} and Eu^{3+}–O^{2-}. Among the 4f excitation transition of Eu^{3+}, the three strong lines correspond to $^7F_0 \rightarrow {}^5L_6$ (395 nm), $^7F_0 \rightarrow {}^5D_2$ (465 nm) and $^7F_0 \rightarrow {}^5D_1$

(536 nm) transitions, which transcend the charge-transfer bands of W^{6+}–O^{2-} and Eu^{3+}–O^{2-}. The relative excitation intensities of the three lines depend on the dopant and dopant concentration. Particularly when Li^+ doped in the host, their relative excitation intensity ratio is dramatically changed and the excitation transitions of the blue and green lines are enhanced obviously. The efficient phosphors (Ca, Eu, M)WO_4 may be promising candidates as red phosphors for white LED.

References

[1] S. Nakamura, T. Mukai, M. Sench, Appl. Phys. Lett. 64 (1994) 1689.
[2] K. Murakam, T. Taguchi, M. Yoshino, Proc. SPIE 4079 (2000) 112.
[3] S. Muthu, F.J. Schuurmans, M.D. Pashley, IEEE J. Sel. Top. Quant. Electron. 8 (2001) 333.
[4] S. Neeraj, N. Kijima, A.K. Cheetham, Chem. Phys. Lett. 387 (2004) 2.
[5] V. Sivakumar, U.V. Varadaraju, J. Electrochem. Soc. 153 (2006) H54.
[6] Z.L. Wang, H.B. Liang, M.L. Gong, et al., Electrochem. Solid-State Lett. 8 (2005) H33.
[7] J.G. Wang, X.P. Jing, C.H. Yan, et al., J. Electrochem. Soc. 152 (2005) G186.
[8] Y.S. Hu, W.D. Zhuang, H.Q. Ye, et al., J. Alloys Compd. 390 (2004) 226.
[9] X.R. Xu, M.Z. Su, Luminescence and Luminescent Materials, Chemical Industry Press, Beijing, 2004, p. 468.
[10] G.J. Blasse, J. Lumin. 72–74 (1997) 129.
[11] M.J. Treadawy, R.C. Powell, J. Chem. Phys. 61 (1974) 4003.
[12] J.k. Tyminski, C.M. Lawson, R.C. Powell, J. Chem. Phys. 77 (1982) 4318.
[13] C.A. Kodaira, H.F. Brito, O.L. Malta, et al., J. Lumin. 101 (2003) 11.
[14] S. Shionoya, W.M. Yen, Phosphor Handbook, CRC Press, 1998, p. 423.
[15] G. Blasse, Prog. Solid State Chem. 18 (1988) 79.